

Studies on the performances of silica aerogel electrodes for the application of supercapacitor

Xuan Du · Chengyang Wang · Tongqi Li · Mingming Chen

Received: 25 July 2008 / Revised: 3 January 2009 / Accepted: 3 January 2009 / Published online: 27 January 2009
© Springer-Verlag 2009

Abstract Silica aerogel (SiO_2 aerogel) was prepared by sol–gel method from tetraethyl orthosilicate hydrolyzation and has been characterized by scanning electron microscopy and N_2 adsorption for its surface structure, surface area, and pore-size distribution. Constant current charge–discharge technique, cyclic voltammetry, and electrochemical impedance spectrum were employed for its specific capacitance and equivalent series resistance. The results showed that the maximum specific capacitance of SiO_2 aerogel electrode in 1 M $\text{Et}_4\text{NBF}_4/\text{PC}$ electrolyte was 62.5 F g^{-1} . In addition, the SiO_2 aerogel capacitor exhibits excellent long-term stability with no significant degradation after 500 charging and discharging cycles. Therefore, the application of high surface area SiO_2 aerogel as electrodes in supercapacitor devices is promising.

Keywords Capacitors · Electrochemical characterizations · Electrodes · Non-aqueous electrolytes · Charging/discharging

Introduction

Supercapacitors are considered as one of the newest innovations in the field of electrical energy storage. They have many attractive characteristics such as low equivalent series

resistance, long charge–discharge life and high power density [1]. The growth in supercapacitors arose from displacing conventional battery and electrolytic capacitor products and from new market applications where existing technologies cannot provide efficient solutions [2]. They can be applied in the hybrid electric vehicle to provide the pulse power for acceleration and recycle the braking energy [2, 3].

Silica aerogels, mesoporous lightweight materials, are currently a field of intensive research activity due to their high potential in a very broad range of applications. Besides structure characteristics, elastic, acoustic, optical, and thermal properties of SiO_2 aerogels have been investigated in detail [4–7]. However, there is no article on the application of SiO_2 aerogels as supercapacitors. SiO_2 aerogels possess structural advantages for electrochemical energy storage as follows: (1) high surface areas ($>500 \text{ m}^2 \text{ g}^{-1}$), which amplify the amount of electrifiable interface [7–9]; (2) mesoporosity, which provides both molecular accessibility and rapid mass transport via diffusion [7, 9–13]; (3) a three-dimensional network of nanometer-sized solid particles, which promotes efficient electronic conduction [9, 10]; and (4) nanoscale particle sizes, which minimize solid-state transport distances for ion-insertion reactions [9, 13]. Based on these features, SiO_2 aerogels can be a desirable material for supercapacitors in organic electrolyte.

In this paper, SiO_2 aerogel was prepared by sol–gel method from tetraethyl orthosilicate (TEOS) hydrolyzation. The electrochemical characteristics of SiO_2 aerogel electrodes in non-aqueous electrolyte have been studied to investigate the application of SiO_2 aerogel as electrodes for electrochemical capacitors.

Experimental

Silica gel was prepared by sol–gel method from TEOS hydrolyzation with several drops of hydrochloric acid as

X. Du · C. Wang (✉) · M. Chen
School of Chemical Engineering and Technology,
Tianjin University,
Tianjin 300072, People's Republic of China
e-mail: cywang@tju.edu.cn

X. Du
e-mail: duxuantd@gmail.com

T. Li
National Key Laboratory of Advanced Functional Composite
Materials, Aerospace Research Institute of Materials
and Processing Technology,
Beijing 100076, People's Republic of China

catalyst according to previous literature [5]. SiO₂ aerogel was obtained after the liquids in the pores of gel were removed through supercritical drying. The density of silica aerogel is 0.093 g cm⁻³.

An automated adsorption apparatus (Quantachrome NOVA 2000, USA) was employed to characterize the surface area and pore size of the SiO₂ aerogel using N₂ adsorption under 77 K. The Brunauer–Emmet–Teller (BET) surface area of SiO₂ aerogel was obtained from N₂ adsorption isotherms and pore-size distribution was obtained by the Barrett–Joyner–Halenda (BJH) theory. The total pore volume was estimated to be the liquid volume of nitrogen at a relative pressure of about 0.99. The average pore diameter was estimated from the surface area and total pore volume. Scanning electron microscopy (SEM) was also used to study the surface structure of the sample.

The electrode for the supercapacitor was prepared in the form of pellets with 80 wt.% content of SiO₂ aerogel, 10 wt.% of acetylene black, and 10 wt.% of PVDF as the binder. The prepared electrodes were dried overnight at 120 °C in vacuum. A unit cell for the capacitor was fabricated with two SiO₂ aerogel electrodes, which have the same mass, separated by a polyethylene membrane using 1 M Et₄NBF₄/PC as electrolyte.

Cyclic voltammetry scans were recorded from 0 to 2.5 V at a scan rate of 1 mV s⁻¹, using CHI604A electrochemical work station (Shanghai, China). Charge–discharge cycle tests were performed using LAND Celltest (Wuhan, China) at a constant current density of 100 mA g⁻¹ with cutoff voltage of 0 to 2.5 V. Electrochemical impedance spectroscopy (EIS) studies were performed on CHI604A electrochemical work station (Shanghai, China) in the frequency range from 100 kHz to 1 mHz.

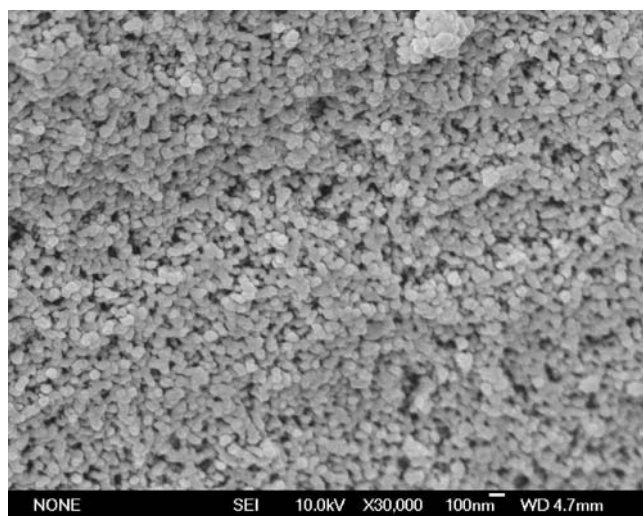


Fig. 1 SEM image of the SiO₂ aerogel

Table 1 Surface characteristics of SiO₂ aerogel

S_P (m ² /g)	S_{micro}/S_P	S_{meso}/S_P	V_P (cm ³ /g)	V_{micro}/V_P	V_{meso}/V_P	D (nm)
904	0.299	0.585	1.68	0.097	0.360	7.43

Results and discussion

SEM images of the surface morphology of the SiO₂ aerogel are depicted in Fig. 1. As being shown in Fig. 1, a large amount of pores exist in the formation of ordered silica aerogel; the silica spheres are all identical with the same diameter. Silica aerogel consists of a three-dimensional network of interconnected silica particles. The silica aerogel with a larger percentage of bigger pores are more suitable to be applied as a non-aqueous supercapacitor electrode because the organic ions are easy of access to the pores [14].

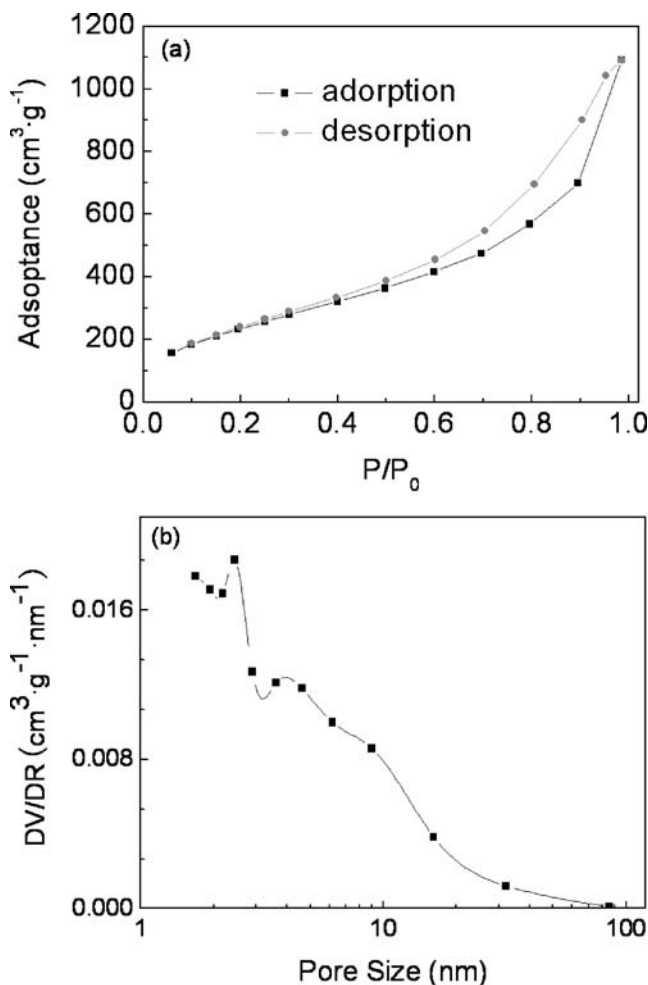


Fig. 2 a The N₂ gas adsorption–desorption isotherm. The squares and circles are adsorption and desorption curve, respectively. b BJH pore size distribution of SiO₂ aerogel

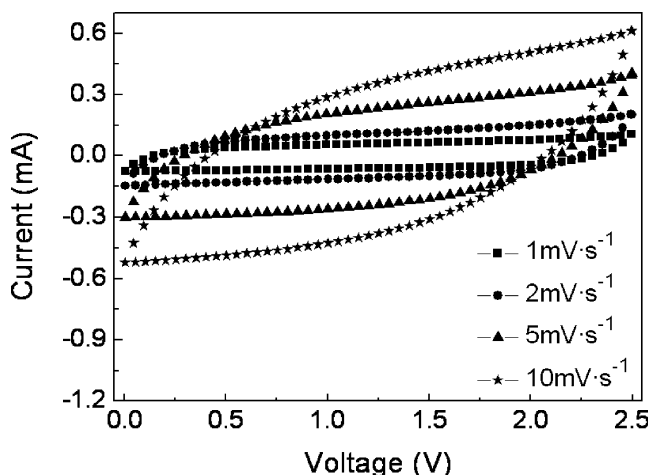


Fig. 3 Cyclic voltammograms of the SiO₂ aerogel electrode in 1 M Et₄NBF₄/PC at different sweep rates

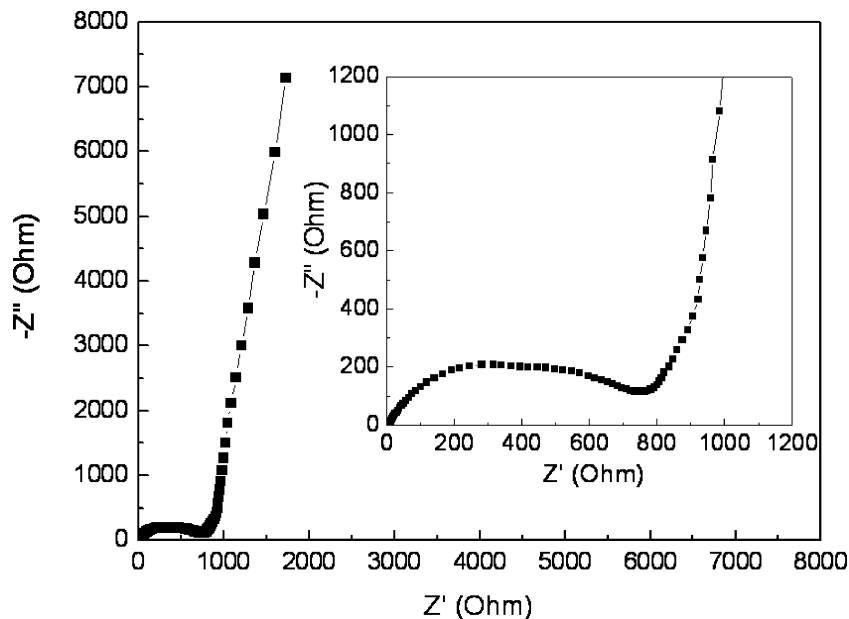
To further investigate the structure of SiO₂ aerogels, the data obtained from BET measurements are summarized in Table 1. According to IUPAC recommendations [15], pores are classified with respect to their size as micropores (width below 2 nm), mesopores (width between 2 and 50 nm), and macropores (width greater than 50 nm). From Table 1, it can be concluded that the SiO₂ aerogel prepared in this study is a typical mesoporous material having a large pore volume and high surface area exceeding 1.6 cm³ g⁻¹ and 900 m² g⁻¹, respectively. In addition, nitrogen sorption isotherms of SiO₂ aerogel and the pore size distribution calculated by BJH method are shown in Fig. 2a and b, respectively. It can be seen from Fig. 2a that the nitrogen adsorption isotherm of type IV (IUPAC classification [15]) is observed like elsewhere [9, 16], exhibiting a clear hysteresis loop arising from capillary condensation of

nitrogen in mesopores. As can be seen from Fig. 2b, silica aerogel has a broad pore size distribution with two peaks at about 2 and 4 nm, respectively. Energy storage in supercapacitors is the accumulation of ionic charge in the double layer at the electrode/electrolyte interface. Hence, the high surface area and the porosity of the SiO₂ aerogel are the basic requirements to achieve the rapid formation of a double layer.

Cyclic voltammetric measurement of the two electrodes was performed in a potential range from 0 to 2.5 V to analyze the electrochemical behavior of the resulting electrodes in 1 M Et₄NBF₄/PC. The voltammograms of the SiO₂ aerogel electrode with sweep rates of 1, 2, 5 and 10 mV s⁻¹ are shown in Fig. 3. It can be seen from the voltammograms that the curves have rectangular-like forms, which is characteristic of an electrical double-layer capacitor. It is suggested that the electrolyte ions can enter into the pores within the electrode to participate in the formation of the electrochemical double layer. Moreover, the voltammograms are very symmetric and smooth, indicating excellent reversibility of the charge–discharge process in the potential range [1]. However, increasing the scan rate enhances the delay of the current to reach a constant value. This arises from the distributed capacitance effects in porous electrodes and the effects are enhanced upon increasing the difference between the ohmic resistance of the electrolyte at the mouth of micropores and that at the bottom of micropores [17].

EIS was further employed to monitor the electrochemical behavior of the electrodes. Electrodes were measured over the frequency range from 100 kHz to 1 mHz at 0 V and the typical Nyquist diagrams for the SiO₂ aerogel electrodes are given in Fig. 4. It can be seen that the capacitors behave as

Fig. 4 Nyquist plots for the supercapacitor based on SiO₂ aerogel



typical capacitors over the frequency range. The intermediate frequency region is the 45° line, which is the characteristic of diffusion into the electrode. In addition, the curve in the figure demonstrated a semicircle at high frequencies and exhibited a straight line which represented the diffusion process of protons in the electrode materials mass and pure capacitance at the low frequency [18].

In order to examine the performance of the resulting SiO₂ aerogel as electrodes in electrochemical supercapacitors, sandwich-type capacitor cells were prepared and subjected to a constant current density of 100 mA g⁻¹ charge–discharge cycling in 1 M Et₄NBF₄/PC media between 0 and 2.5 V. At the same time, the charge–discharge cycling test was conducted 500 times.

The galvanostatic charge–discharge curve conducted at a current density of 100 mA g⁻¹ is given in Fig. 5. As shown in Fig. 5, the current–resistance (IR) drop of the supercapacitor was relatively obvious, which is mainly derived from the low electronic conductivity of the SiO₂ aerogel. Nevertheless, a linear variation of the voltage was observed during the charging–discharging process, which can prove that the supercapacitor has good electrochemical capacitance performance.

The specific charge–discharge capacitance of the electrodes (C) in the cells was determined by Eq. 1 [19].

$$C = 2 \times I / [(dV/dt)\omega] \quad (1)$$

where I and dV/dt , respectively, indicate the constant current that is applied and the slope of these chronopotentiometric curves when the curve is approximately linear and symmetric; ω represents the mass of electroactive material. The factor of 2 originates from the fact that the total capacitance measured from the test cells is the addition of two equivalent single-electrode capacitors in series.

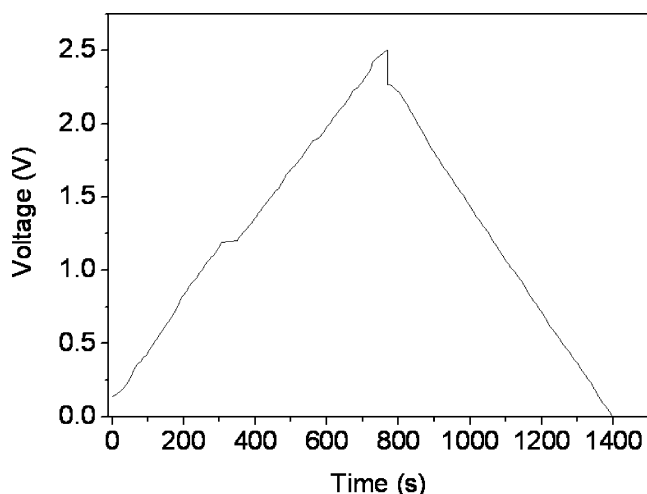


Fig. 5 Charge/discharge curve of the SiO₂ aerogel supercapacitor at 100 mA g⁻¹ in 1 M Et₄NBF₄/PC

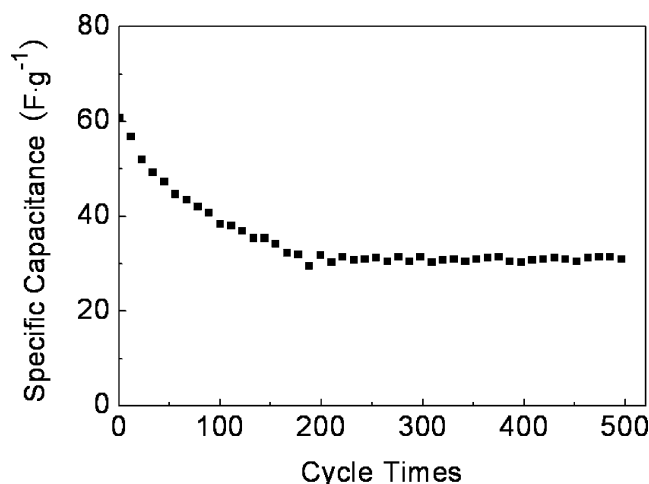


Fig. 6 Variation of capacitance and coulombic efficiency with cycle number for the SiO₂ aerogel capacitor charged and discharged at 100 mA g⁻¹ in 1 M Et₄NBF₄/PC

Based on the experimental results of Fig. 6, it can be found through calculation of Eq. 1 that the highest capacitance of the SiO₂ aerogel-based supercapacitor is up to 62.5 F g⁻¹ and the corresponding specific volume capacitance is 82.8 F cm⁻³. The cycle life of the SiO₂ aerogel supercapacitor is also illustrated in Fig. 6. Although there is a decrease in the specific capacitance in the first 100 cycles, it then remains stable over the rest 400 cycles. The long charge–discharge cycling test indicates the high stability of the SiO₂ aerogel and its potential as an electrode material for long-term capacitor applications. Therefore, SiO₂ aerogel electrodes have excellent charge/discharge characteristics in organic electrolyte.

The Ragone plot of SiO₂ aerogel supercapacitor, which is used to relate the power density to the energy density, is exhibited in Fig. 7. The energy and power densities were calculated by means of constant-current charging–discharging

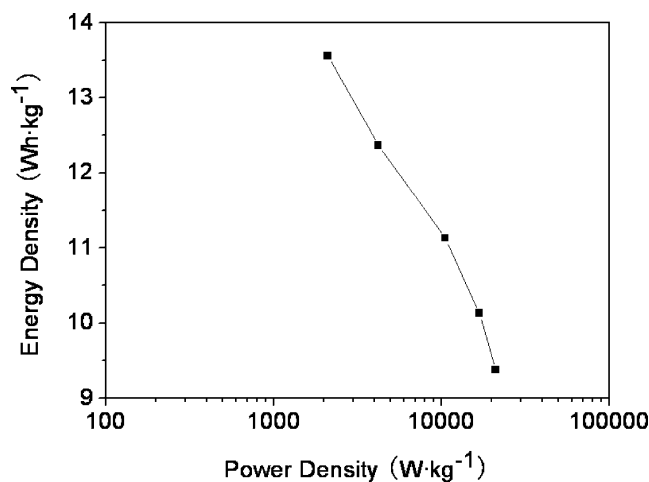


Fig. 7 Ragone plot relating power density to achievable energy density of the SiO₂ aerogel capacitor

of a supercapacitor using a cell-voltage window of 2.5 V and current densities between 100 and 1,000 mA g⁻¹. The energy and power densities can be calculated as following [20]:

$$E = CV^2/2 \quad (2)$$

$$P = iV/2 \quad (3)$$

where C , V , and i are the gravimetric capacitance, the potential at the start of discharge, and the current density, respectively. As observed in Fig. 7, higher energy densities were achieved at the expense of power capability in the SiO₂ aerogel-based supercapacitor. In addition, the energy density decreased with the increase of current density because the electrolyte is hard to access by some pores at higher current density. However, according to the result of Fig. 7, the SiO₂ aerogel-based supercapacitor showed high energy density and power density. Hence, SiO₂ aerogel has the potential to be an active electrode material for supercapacitor.

Conclusions

In this paper, the electrochemical performances of supercapacitors based on SiO₂ aerogel, prepared by sol-gel method, have been investigated for the first time. According to the N₂ adsorption analysis, SiO₂ aerogel studied in this paper are typical mesoporous material and possess high surface area. The specific capacitance of the supercapacitor of about 62.5 F g⁻¹ was obtained using 1 M Et₄NBF₄/PC as the electrolyte. The highly accessible surface area, stable electrochemical properties, excellent reversibility, and the long cycle life of SiO₂ aerogel electrode demonstrate that it

has potential advantages for the fabrication of supercapacitors.

Acknowledgments The authors would like to thank Zhi-ping Ge for the surface area measurements.

References

1. Conway BE (1999) Electrochemical supercapacitors. Kluwer, New York
2. Burke A (2000) *J Power Sources* 91:37–50
3. Frackowiak E, Béguin F (2001) *Carbon* 39:937–950
4. Hrubesh LW (1998) *J Non-Cryst Solids* 225:335–342
5. Yang HL, Ni W, Sun CC et al (2006) *Aerospace Materials and Technology* 2:18–22
6. Gibiat V, Lefevre O et al (1995) *J Non-Cryst Solids* 186:244–255
7. Schmidt M, Schwertfeger F (1998) *J Non-Cryst Solids* 225:364–368
8. Sousa A, Souca EMB (2006) *J Non-Cryst Solids* 352:3451–3456
9. Scherer GW (1998) *J Colloid Interface Sci* 202:399–410
10. Scherer GW, Calas S, Sempere R (1998) *J Colloid Interface Sci* 202:411–416
11. Pekala RW, Farmer JC, Alviso CT et al (1998) *J Non-Cryst Solids* 225:74–80
12. Dong W, Sakamoto JS, Dunn B (2003) *Sci Technol Adv Mater* 4:3–11
13. Anappara AA, Rajeshkumar S, Mukundan P et al (2004) *Acta Materialia* 52:369–375
14. Shi H (1996) *Electrochim Acta* 41:1633–1639
15. Sing KSW, Everett DH, Haul RAW et al (1985) *Pure Appl Chem* 57:603–619
16. Rassy HE, Buisson P, Bouali B et al (2003) *Langmuir* 19:358–363
17. Chen WC, Wen TC, Teng HS (2003) *Electrochim Acta* 48:641–649
18. Arulepp M, Permann L, Leis J et al (2004) *J Power Sources* 133:320–328
19. Li J, Wang X, Huang Q et al (2006) *J Power Sources* 158:784–788
20. Wang DW, Li F, Liu M et al (2008) *Angew. Chem* 47:373–376